



Over 27% efficiency GaAs/InGaAs mechanically stacked solar cell

Hideki Matsubara^{a,*}, Tatsuya Tanabe^a, Akihiro Moto^a,
Yasuo Mine^b, Shigenori Takagishi^a

^a Basic High-Technology Labs, Sumitomo Electric Industries, Ltd. 1-1-1, Koya-kita; Itami Hyogo 664, Japan

^b Systems and Electronics R & D Center, Sumitomo Electric Industries, Ltd. 1-1-1, Koya-kita; Itami Hyogo 664, Japan

Abstract

We have applied an InGaAs solar cell (band gap = 0.75 eV) to the bottom cell of the super-high-efficiency tandem solar cell aiming an over 35% conversion efficiency. The InGaAs cell which is lattice-matched to the InP substrate showed the efficiency of 5.5% under the GaAs substrate with low carrier concentration. Combining with the GaAs cell by means of a mechanically stacking technique, we obtained an efficiency of 28.8% at air mass (AM) 1.5, 1-sun. This result suggests the possibility of the cells with the efficiency of over 35% with combining a GaInP/GaAs monolithic tandem cell and the InGaAs cell (or InGaAsP cell).

Keywords: GaAs/InGaAs; Solar cells; Efficiency

1. Introduction

There have been several reports on GaInP/GaAs monolithic tandem cells with efficiency of almost 30% on the GaAs substrates [1–3]. To achieve the further improvement of conversion efficiency of higher than 30%, the fabrication of a bottom cell with a narrow band gap material is one of the keys. We have progressed our landmark program in order to show the highest potential of the solar cell with compound semiconductors. The goal of this program is to obtain the over 35%

* Corresponding author.

efficiency by a triple-junction super-high efficiency solar cell with the combination of the GaInP/GaAs monolithic tandem cell and the narrow band gap bottom cell. As the first step of this program, we fabricated a mechanically stacked double-junction GaAs/InGaAs solar cell. Fig. 1 shows the schematic view of our GaAs/InGaAs tandem solar cell. In this report, $\text{In}_{0.47}\text{Ga}_{0.53}\text{As}$ (band gap = 0.75 eV) cell which is lattice-matched to a InP substrate is selected as the bottom cell of the tandem cell. InGaAs expects to have a high-photo response in the wide wavelength ranges of 870–1700 nm, even under the GaAs substrate. The mechanically stacking technique is one of the simple fabrication processes to produce the tandem solar cells. With this method solar cells whose lattice-constants are mismatched are easily combined.

Another end of our program is to develop a safer epitaxial growth process for the solar cells with compound semiconductors. The solar cells of GaAs- (or InP-) related compounds are normally fabricated by metalorganics chemical vapor deposition (MOCVD) epitaxial growth process. The conventional MOCVD process uses hazardous hydride gas-phase group-V sources: AsH_3 and PH_3 . Since these sources have high toxicity and are supplied as compressed gases, large and expensive exhaust equipment is needed in the case of unintentional gas diffusion into air. Recently, tertiarybutylarsine (tBAs, $\text{C}_4\text{H}_9\text{AsH}_2$) and tertiarybutylphosphine (tBP, $\text{C}_4\text{H}_9\text{PH}_2$) have been intensively researched because they are liquid phase at room temperature and less toxic than currently used gas sources [4]. We have reported the growth of the GaAs single-junction solar cells with tBAs and tBP and showed their high performance [5–7]. In this report, the GaAs top cell was grown with these safer metalorganics precursors.

2. Experimental

GaAs epitaxial layers for the top cell were grown with triethylgallium (TEGa) and tBAs in a vertical, cold-wall, RF-heated, quartz reactor. Horizontal-Bridgeman-grown GaAs(1 0 0) misoriented 2° toward $\langle 110 \rangle$ substrates were used for the solar cell structure growth. Both sides of the GaAs substrate were mirror-like surfaces, for both sided device fabrication process of the top cell. No pre-etching for the epitaxial growth was required, for the surfaces of the substrates were Sumitomo's Super Clean grade (Epi-ready). The growth pressure was set to 76 Torr. The growth temperature and the V/III ratio were 550°C and 4, respectively. GaInP layers which are lattice-matched to GaAs were grown with TEGa, trimethylindium and tBP for the window and back surface field (BSF) layer of the top cell. The V/III ratio for GaInP layers was set to 50.

On the other hand, InGaAs solar cell structures were grown by the conventional MOCVD using AsH_3 and PH_3 because there remains some difficulty on the InGaAs layer growth by all metalorganics precursors MOCVD at present. Liquid-encapsulated-Czochralski-grown InP(1 0 0) substrates were used for the bottom cell growth. The growth pressure was set to 60 Torr. The growth temperature and the V/III ratio for the InGaAs layers were 650°C and 30, respectively. InP layers which were adopted

to the window and BSF layers of the InGaAs cell were grown under the condition of V/III ratio = 200.

An ordinary photolithography, metal evaporation, and lift-off process were employed for the solar cell fabrication. For combining two cells, the GaAs top cell is attached to a self-made stack holder and stacked on the InGaAs bottom cell without any resin (Fig. 1). In this configuration, top and bottom cells are separated electrically. The solar cell performance under AM1.5 global 1-sun (100 mW/cm^2) was measured with a solar simulator and an I–V curve tracer. Careful calibration was done with the data measured at Japan Quality Assurance Organization(JQA).

3. Results

3.1. Optical transmittance of GaAs substrate

For the ideal performance on the GaAs/InGaAs stacked cell, it is required that the optical transmittance of the GaAs substrate is high at wavelength ranges of 870–1700 nm. We checked the carrier concentration dependence of the transmittance of GaAs substrates because there is free-carrier absorption in conducting GaAs substrates in the wavelength region longer than the band gap energy of GaAs. For this experiment, a silicon solar cell was used as the bottom cell with the same configuration in Fig. 1. Fig. 2 shows the measured short circuit currents (I_{sc}) of the Si bottom cell under GaAs substrates with various carrier concentrations, implying that GaAs substrates with the carrier concentration higher than $1 \times 10^{18} \text{ cm}^{-3}$ have large absorption at the wavelength longer than 870 nm. From the spectral response data, it is found that n-type GaAs substrates with the carrier concentration lower than $5 \times 10^{17} \text{ cm}^{-3}$ have an over 80% transmittance at the wavelength longer than 870 nm. We can be fairly certain that the requirement in fabricating high-efficiency mechanically stacked cell is the use of n-GaAs substrates with the carrier concentration lower than $5 \times 10^{17} \text{ cm}^{-3}$.

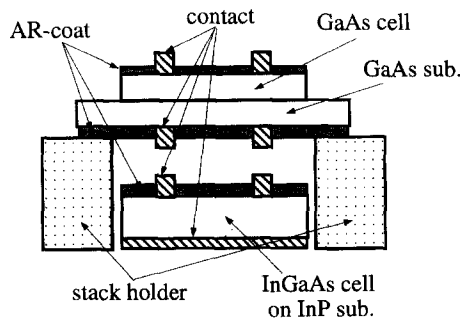


Fig. 1. Schematic view of the mechanically stacked GaAs/InGaAs tandem solar cell.

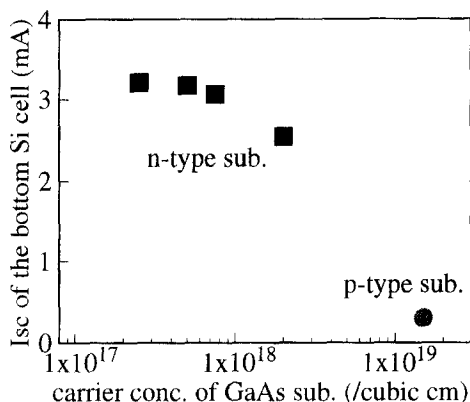


Fig. 2. Carrier concentration dependence of infrared transmittance for GaAs substrates.

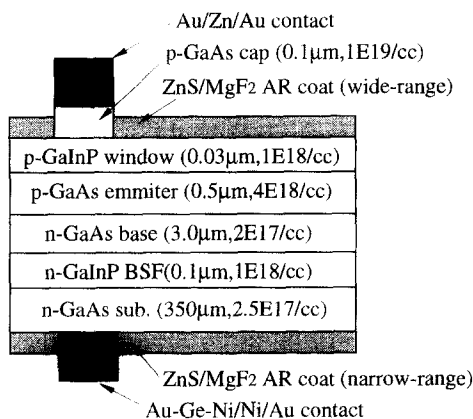


Fig. 3. Structure of the single-junction GaAs top cell.

3.2. GaAs cell performance

Considering the result of the transmittance of GaAs substrates, we chose the p on n-type GaAs cell structure on the n-type GaAs substrate with carrier concentration of $2.5 \times 10^{17} \text{ cm}^{-3}$. Fig. 3 shows the GaAs top cell structure. The lattice-matched GaInP window layer was adopted to the GaAs cell because it was assured with our previous work that the interface recombination velocity (S) at p-GaAs/p-GaInP interface is significantly low (3600 cm/s) and thus the spectral response of the GaAs cell in the short wavelength region (blue response) is quite good [7]. At this time, the GaInP layer was also adopted to the BSF layer of the GaAs cell in order to improve the spectral response in the long wavelength region (red response). The area of the cell was 1 cm^2 , which was defined by mesa-etching. Comb-type metal contacts on the both

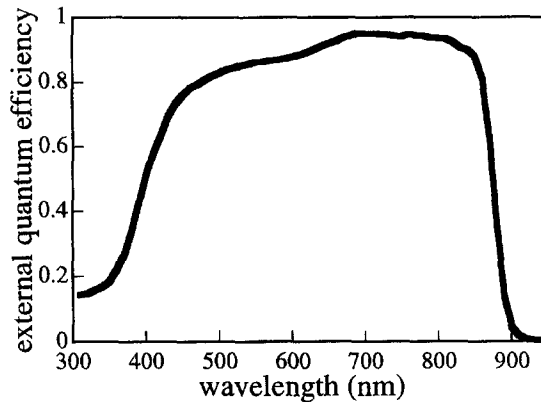


Fig. 4. Spectral response of the GaAs top cell.

sides of the cell were aligned to reduce optical shadow losses by the infrared photo-mask aligner. An alloyed Au/Zn/Au metal for front-side p-type contact, and an alloyed Au–Ge–Ni/Ni/Au metal for back-side contact were employed, respectively. The metal contact coverage was 5% of the total cell area. The region of GaAs cap without metal contact coverage was selectively removed with a buffered $\text{NH}_3\text{--H}_2\text{O}_2$ etchant. Two type double-layer ZnS/MgF₂ antireflection (AR) coats were deposited; the coat for visible and infrared (wide-range type AR; ZnS = 54 nm, MgF₂ = 92 nm) on the front side of the cell, and the coat for infrared (narrow-range type AR; ZnS = 117 nm, MgF₂ = 200 nm) was on the back side of the cell.

The top GaAs cell performance were measured on the stack holder. The open circuit voltage (V_{oc}), I_{sc} , fill factor (FF), and efficiency of the top cell at AM1.5, 1-sun were 1.037 V, 27.8 mA, 0.807, and 23.3%, respectively. The spectral response of the GaAs cell is shown in Fig. 4. Compared with our previous results, I_{sc} of the GaAs cell increased, but FF decreased. The increase of I_{sc} is derived with the improvement of the red response of the cell which attributed to the use of GaInP BSF layer. This result indicates that the S at n-GaAs/n-GaInP interface is very low similar to the p-type interface. The decrease of FF indicates the increase of series resistance in the GaAs top cell. We speculate that the increase of the resistance comes from a low carrier concentration substrate and back side comb-type metal contact. The problem of the lowering FF remains one of the obstacle for constructing super-high efficiency tandem solar cell.

3.3. InGaAs cell performance

The structure of InGaAs bottom cell is shown in Fig. 5. First of all, we compared the p on n-type structure with the n on p-type structure. The cell structures were the same, but only n-type and p-type layers were switched; the front-side emitters were commonly set to 0.4 μm thick and $1 \times 10^{18} \text{ cm}^{-3}$, and the back-side bases were

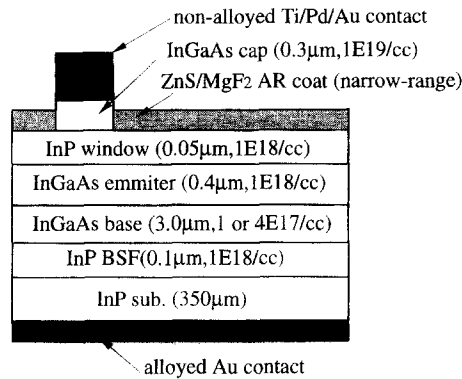


Fig. 5. Structures of the single-junction InGaAs bottom cells.

Table 1

Performance data of the InGaAs bottom cells with various structures. Minority carrier diffusion lengths of the base layers measured by EBIC are also shown

	V_{oc} (V)	I_{sc} (mA)	FF	Eff. (%)	Dif. leng. (μm)
p on n-InGaAsbase c.c.: $1 \times 10^{17} \text{ cm}^{-3}$	0.33	44.0	0.66	9.4	3.5
n on p-InGaAsbase c.c.: $1 \times 10^{17} \text{ cm}^{-3}$	0.37	42.5	0.70	10.9	> 30
n on p-InGaAsbase c.c.: $1 \times 10^{17} \text{ cm}^{-3}$	0.39	42.8	0.71	11.8	> 30

commonly set to $3.0 \mu\text{m}$ thick and $1 \times 10^{17} \text{ cm}^{-3}$. Epitaxial InP layers were adopted to window and BSF layers, expecting low S at InGaAs/InP interfaces. The area of the cells was also 1 cm^2 . The same shaped comb-type metal contacts as the top cell were fabricated on the front side of the InGaAs bottom cells. At either p on n-type or n on p-type, a non-alloyed Ti/Pd/Au metal was used for front-side contact, and an alloyed Au metal for back-side contact was used. The narrow-range type ZnS/MgF₂ AR coat for infrared was deposited on the front side of the cell because the InGaAs bottom cell can perform only in the wavelength range of 870–1700 nm under the GaAs top cell.

Table 1 shows performance data of the InGaAs cells at AM1.5, 1-sun. The V_{oc} of n on p-type cell was higher than that of p on n-type cell. These results coincide with the data reported by Wanlass et al. [8]. In order to investigate the difference, we measured the minority carrier diffusion length (L) of the InGaAs base layers for both cells by means of electron-beam-induced current (EBIC) method. The estimated L 's of the base layers are also presented in Table 1. The p-type InGaAs base layer has much longer minority carrier diffusion length than that of n-type InGaAs base layer. Electrons in the InGaAs has much longer lifetime than holes, and thus the dark

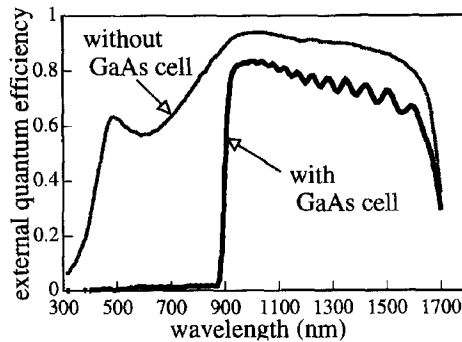


Fig. 6. Spectral responses of the InGaAs bottom cell with or without the GaAs top cell.

saturated current in the p-type InGaAs base should be very low, which results in the higher V_{oc} at the n on p-type cell. This is consistent with our analysis that the mobility of electrons in InGaAs is 50 times larger than that of holes, which is derived with the large difference of effective mass between electrons and holes in InGaAs.

We also changed the carrier concentration of the p-type InGaAs base layer at n on p-type structure. Table 1 also compares the performance data of the low carrier concentration base layer cell ($1 \times 10^{17} \text{ cm}^{-3}$) and high carrier concentration base layer cell ($4 \times 10^{17} \text{ cm}^{-3}$). The data show the V_{oc} of high carrier concentration base layer cell is larger than low carrier concentration base layer cell. This result implies that the Burstein–Moss shift effect in the base layer of InGaAs cell contributes the performance of the cell.

3.4. Mechanically stacked GaAs/InGaAs cell

Finally, we chose the n on p-type InGaAs cell with higher carrier concentration of the base layer as the bottom cell and fabricated a mechanically stacked tandem solar cell. Fig. 6 shows the spectral responses of the InGaAs bottom cell with or without the GaAs top cell described earlier. The conversion efficiency of the InGaAs cell under the GaAs cell was 5.5% ($V_{oc} = 0.365 \text{ V}$, $I_{sc} = 21.7 \text{ mA}$, and $FF = 0.688$). To our knowledge, this is the highest efficiency at the condition of measurement under the GaAs substrate, AM1.5, 1-sun. Therefore, we successfully obtained the total efficiency of 28.8% at AM1.5, 1-sun with the mechanically stacked GaAs/InGaAs tandem cell. It should be concluded that the first step of our program is completed.

4. Further task

In the near future, we will change the bottom cell to an InGaAsP cell with the band gap of 0.95 eV corresponding to the wavelength of 1300 nm. From simple theoretical calculation, the optimum band gap energy of the bottom cell under the GaAs

substrate for the maximum conversion efficiency at AM1.5, 1-sun is found to be 0.95 eV [8]. Furthermore, we will change the top cell to the p on n-type GaInP/GaAs monolithic tandem cell. If we succeed to fabricate a 30% efficiency cell on the n-type GaAs substrate, we will obtain an efficiency of over 35% with mechanically stacked GaInP/GaAs/InGaAsP solar cell. Next challenge is to grow all structures of the super-high-efficiency tandem solar cell by the safer all metalorganics precursors MOCVD method.

Another aspect of our task is to develop a lower cost cell with super-high efficiency. The cost of GaInP/GaAs/InGaAsP solar cell is very high because two kinds of substrates of compound semiconductors are needed. There is, however, one possibility for triple-junction solar cell on a single substrate, because a new low band gap material which is lattice-matched to GaAs discovered in the system of InGaAsN compound [9]. If the InGaAsN is good enough to operate as a minority carrier device, GaInP/GaAs/InGaAsN monolithic tandem cell on single GaAs (or Ge) substrate will be one of attractive candidate for the low-cost, super-high-efficiency solar cell.

Acknowledgements

This work was partially supported by the New Energy and Industrial Technology Development Organization as a part of the New Sunshine Program under the Ministry of International Trade and Industry.

References

- [1] K.A. Bertness, S.R. Kurtz, D.J. Friedman, A.E. Kibbler, C. Krammer, J.M. Olson, Proc. 1st WCPEC, IEEE, 1994 p. 1671.
- [2] P.R. Sharps, M.L. Timmons, Y.C.M. Yeh, C.L. Chu, Proc. 1st WCPEC, IEEE, 1994, p. 1725.
- [3] T. Takamoto, E. Ikeda, H. Kurita, M. Ohmori, Proc. 1st WCPEC, IEEE, 1994, p. 1729.
- [4] C.H. Chen, C.A. Larsen, G.B. Stringfellow, Appl. Phys. Lett. 50 (1987) 218.
- [5] H. Matsubara, A. Saegusa, T. Tanabe, H. Kimura, S. Takagishi, T. Shirakawa, K. Tada, Technical Digest of PVSEC-7, Nagoya, 1993.
- [6] T. Tanabe, H. Matsubara, A. Saegusa, H. Kimura, S. Takagishi, T. Shirakawa, K. Tada, J. Cryst. Growth. 145 (1994) 408.
- [7] H. Matsubara, T. Tanabe, A. Saegusa, S. Takagishi, T. Shirakawa, Proc. 1st WCPEC, IEEE, 1994, p. 1871.
- [8] M.W. Wanlass, J.S. Ward, T.A. Gessert, K.A. Emery, G.S. Horner, T.J. Coutts, G.F. Virshup, M.L. Ristow, Proc. 21st PVSC, IEEE, 1990, p. 172.
- [9] M. Kondow, K. Uomi, A. Niwa, T. Kitatani, S. Watahiki, Y. Yazawa, Jpn. J. Appl. Phys. 35 (1996) 1273.